


 Cite this: *RSC Adv.*, 2024, 14, 27132

# AuAgCu trimetallic nanoparticles based alloy: an advanced electrocatalyst for hydrogen evolution reaction in alkaline media†

 Kanwal Memon, <sup>\*a</sup> Roomia Memon, <sup>\*ab</sup> Zafar Hussain Ibutoto, <sup>c</sup>  
 Ghufran Ahmed Memon, <sup>d</sup> Halar Haleem, <sup>e</sup> Sirajuddin, <sup>f</sup> Ayaz Ali Memon, <sup>a</sup>  
 Anjum Qureshi, <sup>b</sup> Javed H. Niazi, <sup>b</sup> Ahmed Nadeem<sup>g</sup> and Sabry M. Attia<sup>g</sup>

Hydrogen production *via* cost-effective electrochemical water splitting is one of the most promising approaches to confront the energy crisis and to obtain clean fuels with high energy density. To address this concern, herein, we developed a simple one-step synthesis method for creating an AuAgCu trimetallic alloy using aspirin as a capping agent. This alloy shows potential for efficient electrocatalyst for hydrogen evolution reaction. The trimetallic nanoparticles based alloy exhibit an equiaxed grain-like morphology and a face-centred cubic phase. In HER experiments using a 1 M KOH electrolyte, the AuAgCu alloy shows nearly negligible overpotential compared to mono- and bimetallic catalysts, and the Tafel slope was 32.7 mV dec<sup>-1</sup>, which is the lowest ever achieved for alloy-based electrocatalysts and extremely close to a commercially available Pt/C with high stability for 21 days and no decrease in current density in alkaline media. Besides, with excellent HER activity and stability, the trimetallic AuAgCu-modified electrode possessed significant durability for over 1000 cycles in the selected range of potential from 0.5 to 0.8 V at different scan rates from 1 to 100 mV s<sup>-1</sup>. This simple, cost-effective and environmentally friendly methodology can pave the way for the exploitation of mixed metal alloy-based electrocatalysts not only for water splitting but also for other applications, such as fuel cells, lithium-ion batteries and supercapacitors.

 Received 11th August 2024  
 Accepted 13th August 2024

DOI: 10.1039/d4ra05826g

[rsc.li/rsc-advances](https://rsc.li/rsc-advances)

## 1. Introduction

To overcome energy problems, hydrogen is considered an ideal replacement for fossil fuels owing to its extraordinary characteristics, such as high efficiency, cleanliness, non-toxicity, and eco-friendliness.<sup>1–3</sup> Because of these properties, many scientists have focused on hydrogen production. At the industrial level, hydrogen is primarily produced through steam reforming of methane, which yields hydrogen with low purity due to the presence of carbon residues.<sup>4,5</sup> Water splitting is an effective

method for generating pure hydrogen, wherein water electrochemically splits into hydrogen and oxygen.<sup>2,3,6</sup> To facilitate the hydrogen evolution reaction (HER), a catalyst is required to initiate proton reduction and lower the activation energy or overpotential.<sup>7,8</sup> Effective electrocatalysts require a large active surface area for electrode materials and high catalytic activity.<sup>9</sup> The catalyst should also have a high exchange current density and a small Tafel slope.<sup>10</sup> Although Pt-based catalysts are commonly used in hydrogen evolution reactions because of their high catalytic activity and effectiveness,<sup>2</sup> the high cost and limited natural abundance of platinum restrict their applications.<sup>2,6,11</sup> Nowadays, nanotechnology plays a crucial role in catalysts because, at the nanolevel, a decrease in the particle size increases the surface-to-volume ratio and enhances catalytic properties.<sup>12</sup> By utilizing nanotechnology, we can develop nanomaterial-based catalysts that are effective towards the HER and affordable electrocatalysts that enable the commercial production of hydrogen from various water sources.<sup>13,14</sup> Previous studies have reported many catalysts from earth-abundant elements, such as Fe-doped Ni, Co-CC, Mo, W, molybdenum sulfides, carbides, tungsten disulfide (WS<sub>2</sub>), and pinewood-derived carbon (PC).<sup>15–17</sup> Although these alternatives are cheaper, some are corrosive under reaction conditions and exhibit poor intrinsic activity and stability.<sup>7,8,18–20</sup> Metal oxides,

<sup>a</sup>National Centre of Excellence in Analytical Chemistry, University of Sindh, Jamshoro, 76080, Pakistan. E-mail: kanwalmemon51@yahoo.com

<sup>b</sup>Sabancı University, SUNUM Nanotechnology Research and Application Center, Orta Mah. Tuzla, 34956, Istanbul, Turkey. E-mail: roomia.memon@sabanciuniv.edu

<sup>c</sup>Institute of Chemistry, University of Sindh, Jamshoro, 76080, Sindh, Pakistan

<sup>d</sup>Department of Urology, Liaquat University of Medical & Health Sciences, Jamshoro, Pakistan

<sup>e</sup>DITEN Department, University of Genoa, 16145, Italy

<sup>f</sup>HEJ Research Institute of Chemistry, International Center for Chemical and Biological Sciences, University of Karachi, 75270, Pakistan

<sup>g</sup>Department of Pharmacology and Toxicology, College of Pharmacy, King Saud University, Riyadh, 11451, Saudi Arabia

 † Electronic supplementary information (ESI) available. See DOI: <https://doi.org/10.1039/d4ra05826g>


such as NiOx, MnOx, Mg(OH)<sub>2</sub>, and transition metal-doped TiO<sub>2</sub>, are used as electrocatalysts for the HER, but they have limited electronic conductivity.<sup>21,22</sup> In contrast, coinage metal nanoparticles are notable for their excellent physicochemical properties, including quantum confinement and surface effects, making them ideal for catalysis.<sup>23</sup> In nanoscience, multimetallic nanoparticles, especially TMNPs, have received great attention owing to their unique catalytic, electrical and optical properties. They also have synergistic effects between multiple metal elements, which are different from monometallic.<sup>24</sup> In previous studies, several methods have been developed for the synthesis of TMNPs, including the microwave (MW) irradiation method,<sup>25</sup> and microemulsion system,<sup>26</sup> and in most methods, multiple steps are involved.<sup>27</sup> To the best of our knowledge, there is no report on the one-step synthesis of trimetallic AuAgCu nanoparticles for water splitting. This first report introduces efficient, low-cost electrocatalysts for rapid and potential HER. Therefore, to increase the density of active sites and electrical conductivity, we proposed the development of a trimetallic AuAgCu alloy as a highly stable and efficient electrocatalyst for HER in alkaline media. Herein, we report a new combination of a trimetallic nanoparticle-based alloy as a strong catalyst for HER in 1 M KOH at room temperature. The electrocatalyst based on the AuAgCu alloy demonstrated efficient HER activity due to a synergistic effect between the three metals as a supporting co-catalyst material. This combination-based electrode exhibits excellent performance for HER with a Tafel slope of (32.7 mV dec<sup>-1</sup>), which is very close to commercial Pt/C (30 mV dec<sup>-1</sup>) and compatible with practical applications. We believe that the present study provides a safe and clean route for synthesizing efficient electrocatalysts based on mixed metal alloys for future renewable energy and energy harvesting.

## 2. Experimental

### 2.1 Materials

Hydrogen tetrachloroaurate trihydrate (HAuCl<sub>4</sub>·3H<sub>2</sub>O), silver nitrate (AgNO<sub>3</sub>), copper chloride pentahydrate (CuCl<sub>2</sub>·5H<sub>2</sub>O), and aspirin (C<sub>9</sub>H<sub>8</sub>O<sub>4</sub>) were purchased from Sigma-Aldrich. All chemicals were of analytical grade and used without further purification.

### 2.2 Synthesis of Au, Ag, and Cu TMNPs

In this synthesis, 300 μL of aspirin solution (0.01 M) was added to 5 mL of Milli-Q water. Then, 100 μL of each metal solution (1 : 1 : 1), *i.e.*, Au, Ag, and Cu (0.01 M), was mixed into that solution, and the volume was made up to 10 mL. The solution was then heated and stirred for 1.5 hours. Over time, a light purple color appeared, indicating the formation of nanoparticles, as shown in the UV-visible spectra in Fig. 1.

### 2.3 Characterization

The morphology of the trimetallic nanoparticles was evaluated using a TEM-FEI Tecnai G2 TF20 UT equipped with a field emission gun operating at 200 kV and a point resolution of 1.9

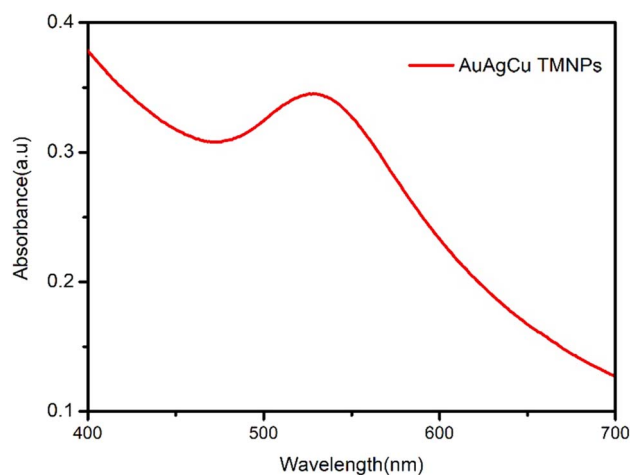


Fig. 1 UV-visible spectra of trimetallic AuAgCu nanoparticles.

Å, along with an energy-dispersive spectrometer (EDS). AFM imaging of the TMNPs was performed using an Agilent 5500 atomic force microscope. The nanocrystalline structure was investigated using X-ray diffraction (XRD) with a Philips PW 1729 diffractometer employing CuK $\alpha$  radiation. A Fourier transform infrared (FTIR) technique was used to determine the interaction between aspirin and trimetallic nanoparticles. The UV-visible spectra were recorded using a Cary Series UV-visible spectrophotometer (Cary 100 UV-vis).

### 2.4 Modification of glassy carbon electrode with synthesized AuAgCu trimetallic alloy nanoparticles

All HER experiments were performed using a Solartron analytical potentiostat with a three-electrode system cell assembly in a 1 M KOH solution with N<sub>2</sub> gas purging. The catalyst ink was prepared by mixing 30 μL of the prepared nanocatalyst and 5 μL of (0.5%) Nafion solution, and the mixture was sonicated in an ultrasonic bath for 15 minutes to obtain the homogenous catalytic ink. A glassy carbon electrode was used for the drop-casting of the nanocatalyst and was used as a working electrode. The modified working electrode was dried with a flow of N<sub>2</sub> gas at room temperature. An Ag/AgCl with saturated KCl as a reference electrode and platinum mesh was used as a counter electrode. Linear sweep voltammetry was used at a scan rate of 1–100 mV s<sup>-1</sup> for HER characterization in alkaline media.

## 3. Results and discussion

### 3.1 Characterization of trimetallic AuAgCu nanoparticles

Fig. 2A–C displays TEM images revealing the unique shape of trimetallic nanoparticles composed of gold (Au), silver (Ag), and copper (Cu). The bright field TEM images showed that the nanoparticles are mainly composed of equiaxed (spherical) grains, with a smaller amount of elongated grains present. This shape is important because it increases the surface area and provides many active sites for reaction, which enhances catalytic performance. The spherical grains offer a high density of reactive sites, while the elongated grains facilitate the



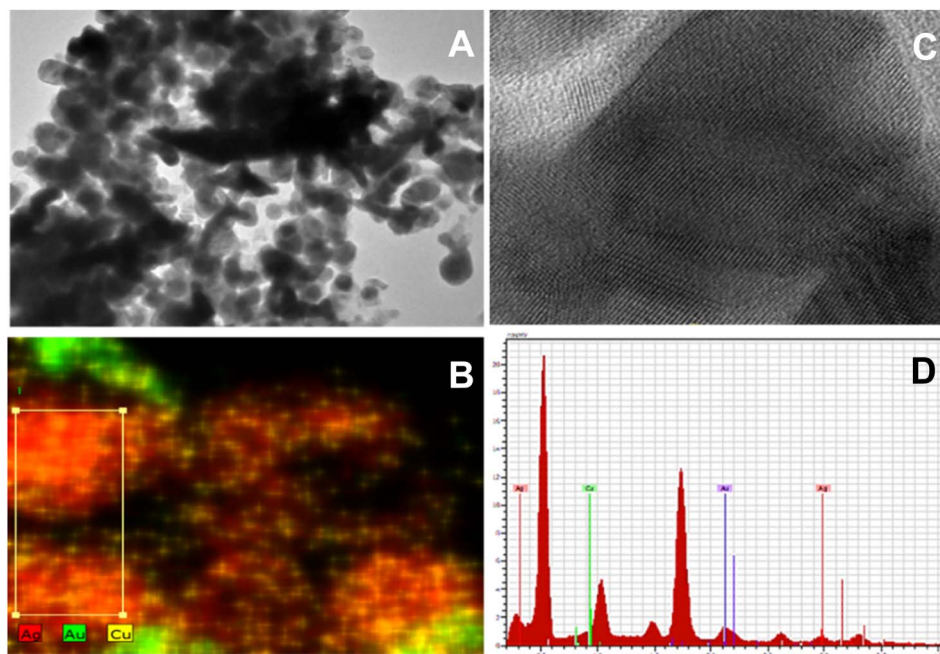


Fig. 2 (A–C) TEM and HR-TEM images of trimetallic nanoparticles, (D) EDS analysis of trimetallic AuAgCu nanoparticles.

movement of reactants and improve mass transport. This unique morphology has significant implications for catalytic applications.

Additionally, the uniform distribution of metals, confirmed by EDS, supports synergistic interactions among Au, Ag, and Cu, further boosting catalytic activity, stability, and selectivity. These structural features and metal distribution combinations make the nanoparticles highly effective for various catalytic processes. EDS also reveals that the former grains consist of Ag with a few Cu (Au free), while the elongated one contains Au and a few % Ag and Cu. Therefore, the sample should be called a nanocomposite of Ag (Cu) binary alloy + Au (Ag, Cu) ternary alloy, as shown in Fig. 2D. XRD study carried out to explore the crystalline nature of nanoparticles. The XRD diffractogram of aspirin-capped trimetallic nanoparticles is shown in ESI S1.† The XRD pattern of the AuAgCu trimetallic nanoparticles shows peaks at  $36.40^\circ$ ,  $42.44^\circ$ ,  $44.26^\circ$  and  $63.5^\circ$ , which are indexed to the (111), (200), (220) and (311) crystal planes of the centred face-centred cubic structure. Peaks appear at (111), (200), (220) and (311), corresponding to the AuAg component. Other peaks at (111), (200) and (220) show the presence of copper (CuO). All peak positions are intermediate to those of AuAg and Cu. The XRD study reveals that the prepared sample of trimetallic nanoparticles does not contain any impurity of  $\text{Cu}_2\text{O}$  or CuO. The XRD results fully agree with the TEM measurements. Fig. 3 shows the AFM image of the trimetallic nanoparticles, which are spherical and uniformly distributed, with an average diameter of 26–35 nm. This morphology, which is coherent with the TEM results, offers a high surface area and prevents clustering, thereby enhancing the availability of active sites for catalytic reactions. The uniform size and distribution contribute to efficient adsorption, interaction with reactants,

and consistent catalytic performance, making these nanoparticles promising for various catalytic applications.

### 3.2 FT-IR analysis

Fourier transform infrared spectroscopy (FTIR) characterization is a convenient and sensitive method for detecting the interaction between two species. In ESI S2-A,† the FT-IR spectra of aspirin are shown, highlighting three main stretchings. The peak appearing at  $2500\text{--}3000\text{ cm}^{-1}$  corresponds to the OH group, while the band at  $1689\text{--}1750\text{ cm}^{-1}$  shows a carbon-oxygen double bond (C=O) and a carbon-oxygen single bond (C-O) confirmed by the appearance of a peak at  $1091\text{--}1304\text{ cm}^{-1}$ . In addition, image S2-B† shows aspirin-capped Au-Ag-Cu TMNPs due to the interaction of aspirin with TMNPs, and the stretching band for carbonyl (C=O) disappears and shifts towards a lower frequency value. This shift confirms the interaction of aspirin with nanoparticles.

### 3.3 EIS analysis

Electrochemical impedance spectroscopy (EIS), another prominent electrochemical technique, verified the conductive and resistive properties of electrodes. EIS typically generates semi-circular peaks in the Nyquist plot, with narrower semicircles indicating higher conductivity and *vice versa*. The EIS study was conducted under optimized conditions, including a quieting time of 2 s, a high frequency of up to 10 000 Hz and a low frequency of 1 Hz at an initial potential of 1.4 V. All the EIS Nyquist plots were circuit fitted, as shown in Fig. 4A and B. In the present study, the AuAgCu/GCE exhibited a narrower semicircle curve than the bimetallic nanoparticles, indicating its exceptional conductive nature and electron transfer from the



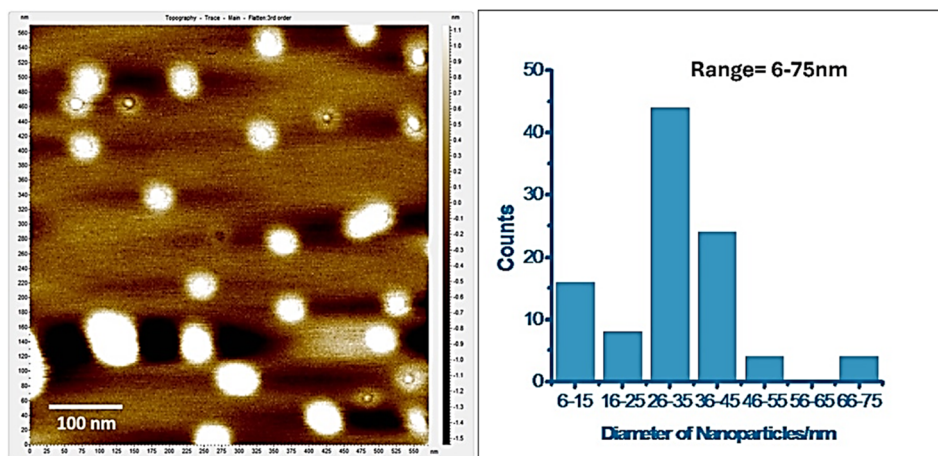


Fig. 3 AFM image of trimetallic AuAgCu nanoparticles.

surface. Overall, the EIS analyses unequivocally demonstrated the excellent conductivity of the AuAgCu trimetallic alloy, making it a promising candidate for utilization as an electrocatalyst for HER reactions.

### 3.4 Electrocatalyst performance of AuAgCu nanoalloy for HER activity

Trimetallic nanoparticles (AuAgCu) were selected as electrocatalysts for the hydrogen evolution reaction (HER). The trimetallic nanoparticles were used for the surface modification of the glassy carbon electrode. The electrode contained a greater contact area between the electrocatalyst materials and sensing species, which enhanced the transport and capture of the target molecules in the electrode and promoted the electron transfer rate. The polarization curves (LSV) for bare glassy carbon electrodes and modified electrodes with trimetallic nanoparticles for measuring HER activity in a 1 M KOH solution are shown in Fig. 5A and B. An AuAgCu catalyst shows nearly negligible overpotential and potential HER activity of these nanoparticles compared to mono and bimetallic nanoparticles.

Entering the HER process, the HER kinetics can be evaluated from the linear region of the Tafel plot by fitting the LSV curve with the Tafel equation as follows:

$$\eta = b \log(j) + a \quad (1)$$

where  $a$  is related to the exchange current density ( $j_0$ ) and  $b$  represents the Tafel slope. Under alkaline conditions, HER kinetics most likely occur *via* the formation of hydrogen-adsorbed intermediates ( $H_{ads}$ ). The formation of  $H_{ads}$  involves electron transfer *via* the discharge of water through the following Volmer step:



Generally, the HER mechanism occurs in three steps: (1) adsorption (Volmer step) (2) desorption (Heyrovsky step), and (3) Tafel slope. All these three steps determine the general rate of reaction.<sup>28</sup> In the first step, hydrogen ions are adsorbed to the surface of the nanoparticles in the second step, hydrogen ions gain electrons to produce hydrogen gas and are discharged from the electrode surface, as shown in the following equations.<sup>29</sup> The HER mechanism on AuAgCu trimetallic alloys is shown in Fig. 6.

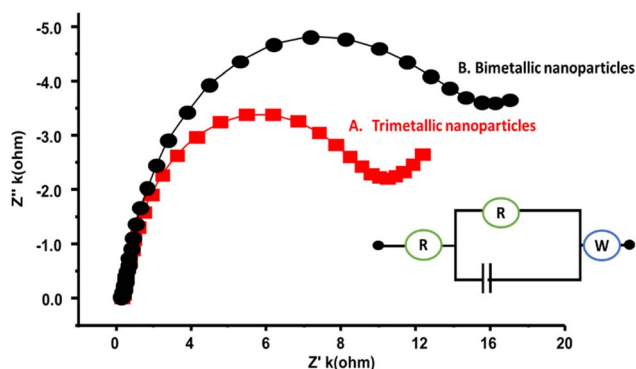
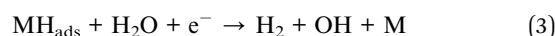


Fig. 4 (A and B) EIS analysis of trimetallic and bimetallic nanoparticles.

Through alkaline water electrolysis, pure hydrogen can be produced, and no emission of carbon residue occurs. The HER Tafel slope is an important step; through this, we determine the reaction mechanism of the catalyst. When the Tafel slope value is high, *i.e.*  $116 \text{ mV dec}^{-1}$ , the discharge step is supposed to be the rate-determining step, and if the Tafel slope value is  $40 \text{ mV dec}^{-1}$ , then the desorption (Volmer–Heyrovsky) is the rate-determining step, or the value of Tafel slope  $30 \text{ mV dec}^{-1}$  indicating the Tafel recombination step (Volmer–Tafel) is the rate-determining step.<sup>30–32</sup> Usually, the small Tafel slopes are useful for practical purposes, as the prepared AuAgCu electrocatalyst exhibits good catalytic activity with a Tafel slope of



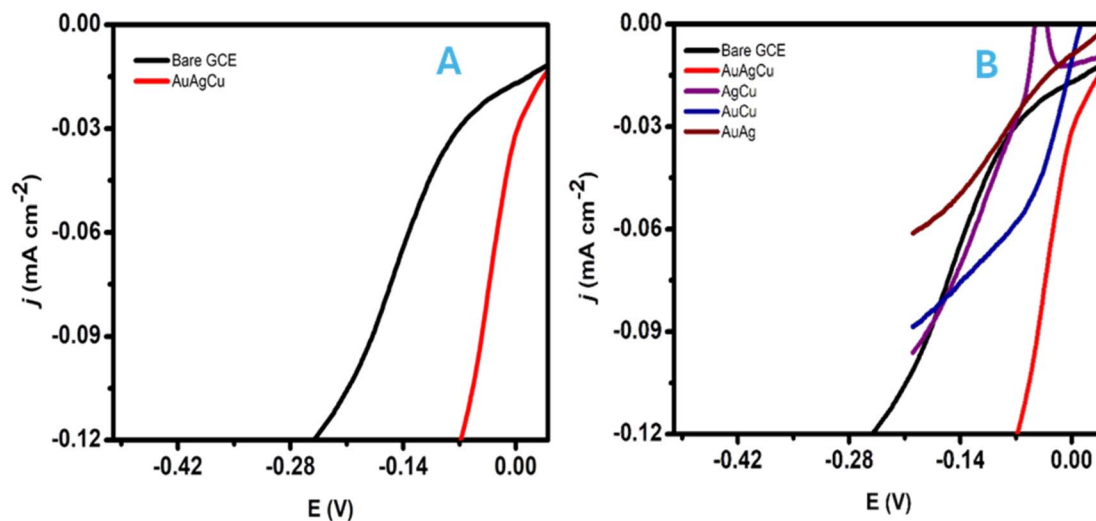


Fig. 5 (A) Linear sweep voltammetry HER polarization curve in  $N_2$ -saturated 1 M KOH at 25 °C of AuAgCu trimetallic nanoparticles, (B) comparison of HER activity of mono-, bi- and trimetallic nanoparticles.

$32.7 \text{ mV dec}^{-1}$ , which is comparable to that of platinum. Fig. 7 shows the Tafel rate-determining step.

### 3.5 Stability of the electrode

An additional key factor is the electrode material's stability. The trimetallic AuAgCu-modified electrode exhibited outstanding HER activity and demonstrated remarkable durability for over 1000 cycles within the selected potential range of 0.5–0.8 V, at various scan rates ranging from 1 to 100  $\text{mV s}^{-1}$ . As depicted in Fig. 8, a small activity is lost and disappears after 1000 cycles.

### 3.6 Reproducibility of the electrode

To investigate the reproducibility of AuAgCu trimetallic nanoalloys, five independent electrodes were modified under similar conditions for measuring HER activity in a 1 M KOH solution, as depicted in Fig. 9. The relative standard deviation of the five modified electrodes was found to be less than 5%, showing acceptable reproducibility. The modified electrodes were kept at room temperature when not in use. After 21 days, no significant change in HER activity was observed, indicating the good chemical and structural stability of the modified electrodes.

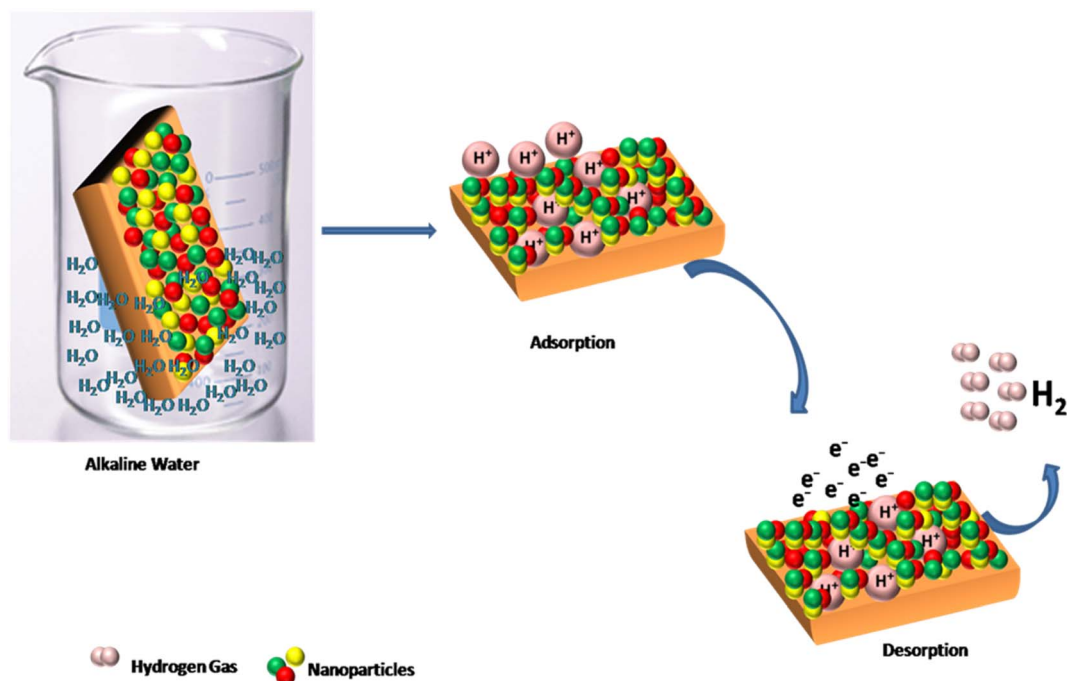


Fig. 6 HER mechanism for water splitting via trimetallic AuAgCu nanoparticles.



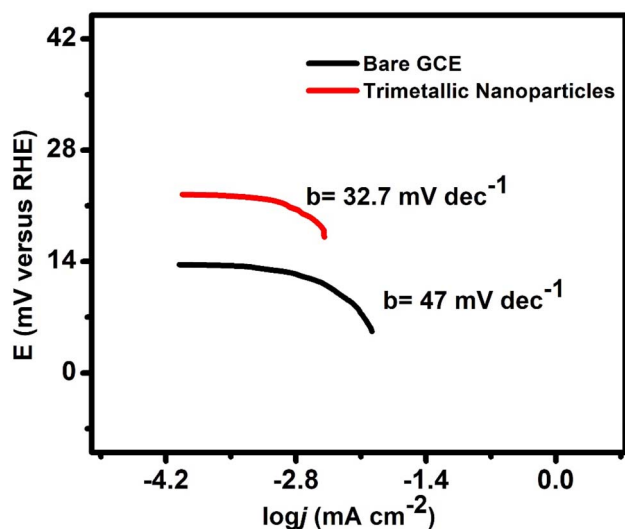


Fig. 7 Calculated Tafel slope of trimetallic AuAgCu nanoparticles.

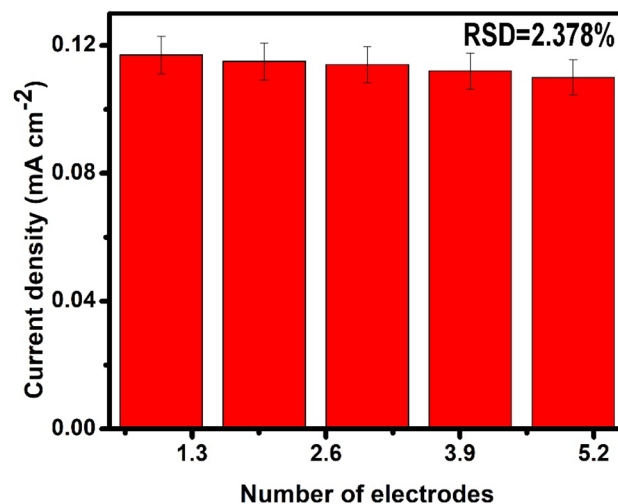


Fig. 9 Reproducibility of synthesized AuAgCu electrodes.

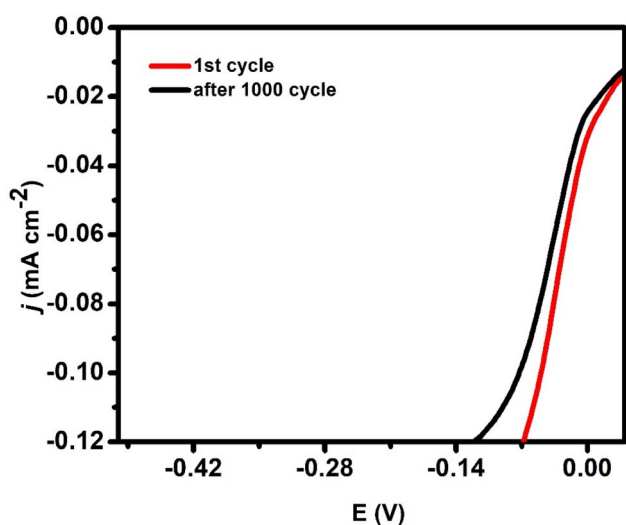


Fig. 8 Stability of the AuAgCu nanoparticle-modified electrode after 1000 cycles.

### 3.7 Discussion

In comparison to AuAgCu metal nanoparticles alloy, very little hydrogen gas was generated at a greater negative overpotential when the HER activity of Au, Ag, and Cu nanoparticles was observed independently. These findings demonstrated the synergistic effect of Ag and Cu in addition to Au, which enhanced the electrochemical evolution of hydrogen. Consequently, the composition of the resulting trimetallic alloy comprises a low quantity of Au with the addition of Ag and Cu. The developed trimetallic alloy performs comparably to Pt/C electrocatalysts sold in stores for the HER. Essential elements of an energetic and catalysis process are the straightforward splitting of reactants to create reaction intermediates and the spontaneous collection of these intermediates. To expose the Ag and Cu features simultaneously, information about the AuAgCu

alloy that is directly related does not need to be optimised. Thus, further investigation of the HER efficiency of trimetallic AuAgCu electrocatalyst is more likely associated with multi-functional aspects, as the edge of Ag permits the splitting of water and the generation of hydrogen intermediates that can be adsorbed close to the surface of Au and recombine into diatomic hydrogen. Moreover, Cu atoms have the tendency to lower the energy barrier needed to build hydrogen intermediates, which makes it easier for them to desorb from their surface and speeds up the rate at which electrons transfer with significantly improved hydrogen evolution performance. The electronic structure of the Au-rich surface in the trimetallic AuAgCu alloy, which prevents transition metal solubility and generates additional surface activities, is one possible reason for the increased HER activity. The decrease in Au 4f binding energies can be attributed to inadequate oxygen binding strength, which is supported by the greatly improved electron coupling interaction between Au, Ag, and Cu. Overall, it was determined that the inner contact of the trimetallic alloys between the Au, Ag, and Cu sections greatly speeds up the reclaim of Au sites for possible electrochemical activity towards HER performance.<sup>30–39</sup> As shown in Table 1, the outcomes produced with these trimetallic alloys are outstanding and comparable to those of the commercial Pt/C catalyst.

### 3.8 Comparative study

This study compared the efficiency of various nanoparticles in alkaline media for hydrogen evolution reactions (HER). The findings are summarized in Table 1. Among the catalysts studied in alkaline media, CuTi (110 mV dec<sup>-1</sup> in 0.1 M KOH),<sup>33</sup> Cu<sub>x</sub>Ni<sub>1-x</sub>SbI (84 mV dec<sup>-1</sup> in 1 M KOH),<sup>34</sup> ReS<sub>2</sub> (170 mV dec<sup>-1</sup> in 1 M KOH)<sup>35</sup> and Mn–Ni<sub>3</sub>Se<sub>2</sub> (167 mV dec<sup>-1</sup> in 1 M KOH)<sup>36</sup> demonstrate reduced efficiency with high Tafel slopes. Additionally, NiP (122 mV dec<sup>-1</sup> in 3 M KOH),<sup>37</sup> Cu<sub>2</sub>CoSnS<sub>4</sub> (110 mV dec<sup>-1</sup> in 1 M KOH),<sup>38</sup> and CuS/NiO (119 mV dec<sup>-1</sup> in 1 M KOH)<sup>39</sup> show slower reaction kinetics and less favourable performance under basic conditions. The commercial Pt/C catalyst exhibits



Table 1 Comparative study of the Tafel slope for various nanoparticles

Different metal combinations	Tafel plot (mV dec <sup>-1</sup> )	Electrolyte	Ref.
CuTi	110	0.1 M KOH	33
Cu <sub>x</sub> Ni <sub>1-x</sub> S. Bi	84	1 M KOH	34
ReS <sub>2</sub>	170	1 KOH	35
NiP	122	3 M KOH	37
Cu <sub>2</sub> CoSnS <sub>4</sub>	110	1 M KOH	38
CuS/NiO	119	1 M KOH	39
Mn-Ni <sub>3</sub> Se <sub>2</sub>	167	1 M KOH	36
Pt/C	30	1 M KOH	11
AuAgCu	32.7	1 M KOH	This work

a low Tafel slope of 30 mV dec<sup>-1</sup> in 1 M KOH, highlighting its high catalytic activity under alkaline conditions but emphasizing the challenges of its cost and scarcity for large-scale applications. The synthesized AuAgCu nanoparticles stand out with a Tafel slope of 32.7 mV dec<sup>-1</sup> in 1 M KOH, demonstrating great efficiency in alkaline media, which potentially offers a more cost-effective alternative to the commercial Pt/C catalyst. The low Tafel slope of AuAgCu nanoparticles indicates their ability to facilitate rapid reaction kinetics and efficient electron transfer in basic environments. The trimetallic composition of Au, Ag, and Cu likely contributes to a synergistic effect, enhancing both catalytic activity and stability. This breakthrough underscores the potential of AuAgCu nanoparticles as highly efficient and economical alternatives to platinum-based catalysts, demonstrating the innovative and impactful nature of the current research.

## 4. Conclusion

In summary, the AuAgCu alloy is synthesized using the wet chemical method in one step. The as-obtained trimetallic nonprecious alloy catalyst exhibited potential HER activity with negligible overpotential and a Tafel slope of 32.7 mV dec<sup>-1</sup> in a 1 M KOH solution. The efficient catalytic activity can be attributed to the mixed metal alloy AuAgCu, in which different elemental constituents could work due to the synergic effect. It can be assumed that the trimetallic alloy would be of great interest as a catalyst in the field of energy harvesting and renewable energy. In addition, the composition of the prepared trimetallic alloy as a favourable material for HER opens a new avenue for the engineering of cost-effective and potential electrocatalysts.

## Data availability

Data supporting the findings of this study are available in this article and its ESI materials.† Additional datasets used and/or analyzed in this study are available from the corresponding author upon reasonable request.

## Author contributions

Kanwal Memon, research and writing – original draft, Roomia Memon data curation, Zafar Hussain Ibupoto conceptualization and methodology, Ghufuran Ahmed Memon, Halar Haleem software and data validation, Sirajuddin writing – editing, Ayaz Ali Memon, formal analysis, Anjum Qureshi, resources, Javed H. Niazi, resources, Sabry M Attia and Ahmed Nadeem investigation.

## Conflicts of interest

The authors declare that there are no conflicts of interest associated with this research.

## Acknowledgements

The authors acknowledge and extend their appreciation to the Researchers Supporting Project Number (RSP2024R124) King Saud University, Riyadh, Saudi Arabia.

## References

- 1 X. Meng, L. Yang, N. Cao, C. Du, K. Hu, J. Su, *et al.*, Graphene-Supported Trimetallic Core-Shell Cu@CoNi Nanoparticles for Catalytic Hydrolysis of Amine Borane, *ChemPlusChem*, 2014, 79(2), 325–332.
- 2 F. Lai, Y.-E. Miao, Y. Huang, Y. Zhang and T. Liu, Nitrogen-Doped Carbon Nanofiber/Molybdenum Disulfide Nanocomposites Derived from Bacterial Cellulose for High-Efficiency Electrocatalytic Hydrogen Evolution Reaction, *ACS Appl. Mater. Interfaces*, 2015, 3558–3566.
- 3 M. Gong, W. Zhou, M.-C. Tsai, J. Zhou, M. Guan, M.-C. Lin, *et al.*, Nanoscale nickel oxide/nickel heterostructures for active hydrogen evolution electrocatalysis, *Nat. Commun.*, 2014, 5, 4695.
- 4 T. K. Townsend, E. M. Sabio, N. D. Browning and F. E. Osterloh, The Hydrogen Evolution Reaction: Water Reduction Photocatalysis—Improved Niobate Nanoscroll Photocatalysts for Partial Water Splitting, *Inorganic Metal Oxide Nanocrystal Photocatalysts for Solar Fuel Generation from Water*, Springer, 2014, pp. 9–25.
- 5 M. Gong, D.-Y. Wang, C.-C. Chen, B.-J. Hwang and H. Dai, A mini review on nickel-based electrocatalysts for alkaline hydrogen evolution reaction, *Nano Res.*, 2015, 1–19.
- 6 X. Zhao, H. Zhu and X. Yang, Amorphous carbon supported MoS<sub>2</sub> nanosheets as effective catalysts for electrocatalytic hydrogen evolution, *Nanoscale*, 2014, 6(18), 10680–10685.
- 7 H. Lv, Z. Xi, Z. Chen, S. Guo, Y. Yu, W. Zhu, *et al.*, A New Core/Shell NiAu/Au Nanoparticle Catalyst with Pt-like Activity for Hydrogen Evolution Reaction, *J. Am. Chem. Soc.*, 2015, 137(18), 5859–5862.
- 8 S. Yu, J. Kim, K. R. Yoon, J.-W. Jung, J. Oh and I.-D. Kim, Rational Design of Efficient Electrocatalysts for Hydrogen Evolution Reaction: Single Layers of WS<sub>2</sub> Nanoplates Anchored to Hollow Nitrogen-Doped Carbon Nanofibers, *ACS Appl. Mater. Interfaces*, 2015, 7(51), 28116–28121.



- 9 A. Iacob, M. Dan, A. Kellenberger and N. Vaszilcsin, Hydrogen evolution reaction on nickel-based platinum electrodes, *Chem. Bull. "Politehnica" Univ. Timisoara*, 2014, **59**(73), 2.
- 10 P. C. K. Vesborg, B. Seger and I. Chorkendorff, Recent Development in Hydrogen Evolution Reaction Catalysts and Their Practical Implementation, *J. Phys. Chem. Lett.*, 2015, **6**(6), 951–957.
- 11 X. Cao, Y. Han, C. Gao, Y. Xu, X. Huang, M. Willander, *et al.*, Highly catalytic active PtNiCu nanochains for hydrogen evolution reaction, *Nano Energy*, 2014, **9**, 301–308.
- 12 E. Serrano, G. Rus and J. Garcia-Martinez, Nanotechnology for sustainable energy, *Renewable Sustainable Energy Rev.*, 2009, **13**(9), 2373–2384.
- 13 X. Qu, P. J. J. Alvarez and Q. Li, Applications of nanotechnology in water and wastewater treatment, *Water Res.*, 2013, **47**(12), 3931–3946.
- 14 H.-L. Wang, J.-M. Yan, Z.-L. Wang and Q. Jiang, One-step synthesis of Cu@FeNi core-shell nanoparticles: Highly active catalyst for hydrolytic dehydrogenation of ammonia borane, *Int. J. Hydrogen Energy*, 2012, **37**(13), 10229–10235.
- 15 J. Liang, Z. Cai, Z. Li, Y. Yao, Y. Luo, S. Sun, *et al.*, Efficient bubble/precipitate traffic enables stable seawater reduction electrocatalysis at industrial-level current densities, *Nat. Commun.*, 2024, **15**(1), 2950.
- 16 C. Tang, R. Zhang, W. Lu, L. He, X. Jiang, A. M. Asiri, *et al.*, Fe-doped CoP nanoarray: a monolithic multifunctional catalyst for highly efficient hydrogen generation, *Adv. Mater.*, 2017, **29**(2), 1602441.
- 17 J. Tian, Q. Liu, A. M. Asiri and X. Sun, Self-supported nanoporous cobalt phosphide nanowire arrays: an efficient 3D hydrogen-evolving cathode over the wide range of pH 0–14, *J. Am. Chem. Soc.*, 2014, **136**(21), 7587–7590.
- 18 Q. Lu, G. S. Hutchings, W. Yu, Y. Zhou, R. V. Forest, R. Tao, *et al.*, Highly porous non-precious bimetallic electrocatalysts for efficient hydrogen evolution, *Nat. Commun.*, 2015, **6**(1), 6567.
- 19 F. Safizadeh, E. Ghali and G. Houlachi, Electrocatalysis developments for hydrogen evolution reaction in alkaline solutions—A Review, *Int. J. Hydrogen Energy*, 2015, **40**(1), 256–274.
- 20 Y. Zheng, Y. Jiao, Y. Zhu, L. H. Li, Y. Han, Y. Chen, *et al.*, Hydrogen evolution by a metal-free electrocatalyst, *Nat. Commun.*, 2014, **5**(1), 3783.
- 21 V. Viswanathan, K. L. Pickrahn, A. C. Luntz, S. F. Bent and J. K. Nørskov, Nanoscale Limitations in Metal Oxide Electrocatalysts for Oxygen Evolution, *Nano Lett.*, 2014, **14**(10), 5853–5857.
- 22 J. Liang, Z. Cai, X. He, Y. Luo, D. Zheng, S. Sun, *et al.*, Electroreduction of alkaline/natural seawater: Self-cleaning Pt/carbon cathode and on-site co-synthesis of H<sub>2</sub> and Mg hydroxide nanoflakes, *Chem*, 2024, DOI: [10.1016/j.chempr.2024.05.018](https://doi.org/10.1016/j.chempr.2024.05.018).
- 23 S. Sareen, V. Mutreja, S. Singh and B. Pal, Highly dispersed Au, Ag and Cu nanoparticles in mesoporous SBA-15 for highly selective catalytic reduction of nitroaromatics, *RSC Adv.*, 2015, **5**(1), 184–190.
- 24 P. Qiao, S. Xu, D. Zhang, R. Li, S. Zou, J. Liu, *et al.*, Sub-10 nm Au–Pt–Pd alloy trimetallic nanoparticles with a high oxidation-resistant property as efficient and durable VOC oxidation catalysts, *Chem. Commun.*, 2014, **50**(79), 11713–11716.
- 25 A. Q. Mugheri and A. A. Otho, Recent Progress in Cost-effective and Stable AuAg/Cu-nanostructured Catalyst for Electrochemical Water Splitting, *Appl. Sci. Conver. Technol.*, 2021, **30**(2), 65–69.
- 26 H. B. Erdem and S. Çetinkaya, AgNi/PC bimetallic and AgNi/PC@Mn trimetallic nanocatalysts for the efficient reduction of 4-nitrophenol, *Catal. Commun.*, 2024, **187**, 106885.
- 27 Y. Zheng, Y. Jiao, Y. Zhu, L. H. Li, Y. Han, Y. Chen, *et al.*, Hydrogen evolution by a metal-free electrocatalyst, *Nat. Commun.*, 2014, **5**(1), 3783.
- 28 T. Shinagawa, A. T. Garcia-Esparza and K. Takanebe, Insight on Tafel slopes from a microkinetic analysis of aqueous electrocatalysis for energy conversion, *Sci. Rep.*, 2015, **5**, 13801.
- 29 B. Pierozynski, On the hydrogen evolution reaction at nickel-coated carbon fibre in 30 wt.% KOH solution, *Int. J. Electrochem. Sci.*, 2011, **6**, 63–77.
- 30 Y. Zheng, Y. Jiao, Y. Zhu, L. H. Li, Y. Han, Y. Chen, *et al.*, Hydrogen evolution by a metal-free electrocatalyst, *Nat. Commun.*, 2014, **5**(1), 3783.
- 31 M. Tavakkoli, T. Kallio, O. Reynaud, A. G. Nasibulin, C. Johans, J. Sainio, *et al.*, Single-Shell Carbon-Encapsulated Iron Nanoparticles: Synthesis and High Electrocatalytic Activity for Hydrogen Evolution Reaction, *Angew. Chem., Int. Ed.*, 2015, **54**(15), 4535–4538.
- 32 W.-F. Chen, J. T. Muckerman and E. Fujita, Recent developments in transition metal carbides and nitrides as hydrogen evolution electrocatalysts, *Chem. Commun.*, 2013, **49**(79), 8896–8909.
- 33 Q. Lu, G. S. Hutchings, W. Yu, Y. Zhou, R. V. Forest, R. Tao, *et al.*, Highly porous non-precious bimetallic electrocatalysts for efficient hydrogen evolution, *Nat. Commun.*, 2015, **6**(1), 6567.
- 34 N. Trivedi, M. Balal, V. Patel, S. R. Barman, C. Sumesh and P. M. Pataniya, Enhanced electrocatalytic performance of Cu<sub>x</sub>Ni<sub>1-x</sub>S Nanoflakes for overall water splitting, *J. Electroanal. Chem.*, 2023, **944**, 117648.
- 35 Q. Zhu, Y. Qu, D. Liu, K. W. Ng and H. Pan, Two-dimensional layered materials: high-efficient electrocatalysts for hydrogen evolution reaction, *ACS Appl. Nano Mater.*, 2020, **3**(7), 6270–6296.
- 36 A. M. Shah, K. H. Modi, P. M. Pataniya, K. S. Joseph, S. Dabhi, G. R. Bhadu, *et al.*, Self-Supported Mn-Ni<sub>3</sub>Se<sub>2</sub> Electrocatalysts for Water and Urea Electrolysis for Energy-Saving Hydrogen Production, *ACS Appl. Mater. Interfaces*, 2024, **16**(9), 11440–11452.
- 37 P. J. Sharma, K. H. Modi, P. Sahatiya, C. Sumesh and P. M. Pataniya, Electroless deposited NiP-fabric electrodes for efficient water and urea electrolysis for hydrogen production at industrial scale, *Appl. Surf. Sci.*, 2024, **644**, 158766.



- 38 K. K. Joshi, P. M. Pataniya, G. R. Bhadu and C. Sumesh, Cu<sub>2</sub>CoSnS<sub>4</sub> electrocatalyst embedded paper working electrodes for efficient, stable, pH universal, and large-current-density hydrogen evolution reaction, *Int. J. Hydrogen Energy*, 2024, **49**, 829–842.
- 39 H. K. Thakkar, K. K. Joshi, P. M. Pataniya, G. Bhadu, S. Siraj, P. Sahatiya, *et al.*, Photo-sensitive CuS/NiO heterostructure electrocatalysts for energy-saving hydrogen evolution reaction at all pH conditions, *Int. J. Hydrogen Energy*, 2023, **48**(97), 38266–38278.

